Effects of Fiber Content on Mechanical Properties of UHPFRC with Coarse Aggregates

Author(s) & Affiliation:

Y.Y.Y. Cao*(corresponding author)- Department of the Built Environment, Eindhoven University of Technology, 5600 MB Eindhoven, the Netherlands, Email: y.cao.1@tue.nl

Q.L. Yu- Assistant Professor, Department of the Built Environment, Eindhoven University of Technology, P.O. Box 513, 5600 MB Eindhoven, the Netherlands, Email: q.yu.1@tue.nl

P.P. Li- Department of the Built Environment, Eindhoven University of Technology, 5600 MB Eindhoven, the Netherlands, Email: p.li@tue.nl

H.J.H. Brouwers- Professor, Department of the Built Environment, Eindhoven University of Technology, P.O. Box 513, 5600 MB Eindhoven, the Netherlands, Email: jos.brouwers@tue.nl

Abstract: Ultra-High Performance Fiber Reinforced Concrete (UHPFRC) is a relatively new construction material with superior mechanical properties. The addition of fibers in UHPFRC has been recognized to significantly enhance its tensile strength, post-cracking ductility and energy absorption capacity. This study investigates the influence of fiber content on the mechanical properties of UHPFRC with coarse aggregates. By applying the Brouwers design method, UHPFRC with a maximum particle size of 8 mm is achieved. The incorporation of coarse basalt aggregates reduces the powder volume fraction in the matrix, and hence brings economic and environmental benefits. Experiments are conducted to investigate the effects of fiber content on the tensile and compressive strengths, as well as the flexural behavior of the UHPFRC. The results show that the compressive strength of the UHPFRC is almost independent on the fiber content. On the contrary, the tensile and the flexural strengths are significantly increased with the increase of the fiber content, and consequently the toughness of the UHPFRC composite has a prominent enhancement with the addition of the steel fibers as well.

Keywords: Ultra-high Performance Concrete, fiber content, performance evaluation, mix design, coarse aggregate

1. Introduction

Ultra-High Performance Fiber Reinforced Concrete (UHPFRC) is a relatively new building material with excellent mechanical strength and durability. To achieve an ultra-high compressive strength (usually around 150 MPa), traditional UHPFRC matrix is usually designed with only fine aggregates and contains a high content of binder [1]. This, however, results in a high production cost and limits the application of UHPFRC [1]. Utilizing cheaper coarse aggregates in UHPFRC is one of the solutions to improve its economic benefit. Moreover, current studies show that UHPFRC with an appropriate content of coarse aggregates possess advantages, and the negative effects resulted from adding coarse aggregates can be prevented by properly packing the granular constituents [2,3]. For instance, Ma et al. [4] reported that the inclusion of coarse aggregates improves the elastic modulus of Ultra-High Performance Concrete (UHPC), benefits its workability and promotes a better shrinkage performance. Researches of [3,5] also presented that the addition of coarse aggregates would not reduce the compressive strength of UHPFRC, and they even observed a slightly higher strength in their studies.

Incorporating steel fibers in UHPFRC contributes to its strength enhancement [6]. Mechanisms of the fiber's effects on UHPFRC can be explained as follows. When an initial micro-crack occurs in the matrix, the presence of the fiber restricts its initiation [7]; as the crack width increases, the fibers effectively bridges between the crack surfaces, inhibit crack propagation, and hence act as sources of strength and ductility [8]. Fiber content is an important factor influencing the tensile strength of UHPFRC. Wille et al. [9] investigated the properties of UHPFRC under direct tension with fiber volume fractions from 1.5% to 3.0%, and their results revealed the strong dependency of the tensile behavior on the fiber content. Similar results were obtained by Abbas et al. [10], which explored the effects of the fiber content (1%, 3% and 6%) on the mechanical properties of UHPFRC. In their study, significant increase in splitting tensile strength was observed with the increase of the fiber content as a consequence of the more effective control for cracking. Nevertheless, most studies about fibers effects concern traditional UHPFRC with only fine aggregates, while the effects on the UHPFRC with coarse aggregates incorporated are still not fully understand.

In this study, UHPFRC containing coarse basalt aggregates is designed using the Brouwers method. The effects of fiber content on the tensile and compressive strengths, as well as the flexural behavior of the UHPFRC are investigated by experiments. This study contributes to the reduction of binders in UHPFRC and promotes to a better understanding about fibers effects on UHPFRC.

2. Testing Methods.

2.1. Materials and mix design

Recipe of the UHPFRC matrix is presented in Table 1.The raw materials used for the UHPFRC mixture are Portland Cement CEM I 52.5 R (CEM), limestone powder (LP), micro-silica (mS), sand (S), basalts aggregate (BA), water (W), superplasticizer (SP) and smooth straight steel fiber (SF) with length = 13 mm, diameter = 0.2 mm, tensile strength = 2750 MPa. The specific densities of the ingredients, particle morphologies and chemical compositions of the used powders can be found in [11]. The fiber contents V_f studied in this research are 0%, 1% and 2% (volume fraction). The amount of superplasticizer is adjusted with the fiber content [12] until a flowability around 20 cm is achieved (measured with Hägermann cone in accordance with EN 1015-3 [13]).

Table 1 Recipe of UHPFRC matrix

Materials	CEM (kg/m^3)	LP (kg/m^3)	mS (kg/m^3)	S (kg/m^3)	BA 2-5 (kg/m^3)	BA 5-8 (kg/m^3)	W (kg/m^3)	SP (kg/m^3)	SF (%)
Quantity	588	156.8	39.2	839.9	413.2	232.3	157	5.0	0
								8.0	1
								17.0	2

It can be noticed that the binder amount utilized in the developed UHPFRC is relatively low, contributing to the environmental sustainability and the economic efficiency. The coarse basalt aggregates applied have two size groups namely 2-5 mm and 5-8 mm, the fraction of which are calculated applying the Brouwers mix design method [14–16]:

$$P_t(D) = \frac{D^q - D_{min}^q}{D_{max}^q - D_{min}^q} \tag{1}$$

$$RSS = \sum_{i=1}^{n} \left[P_m(D_i) - P_t(D_i) \right]^2 \rightarrow \min \tag{2}$$

where D, D_{min} and D_{max} represent the particle size and the minimum and maximum values, respectively. q is the distribution modulus, and q = 0.22 is recommended in [17] for UHPFRC. $P_t(D)$ is the cumulative fraction of the total solid with a size smaller than D, in which the lower corner mark t denotes the target percentage. P_{m} presents the cumulative fraction of the designed mix. Optimization algorithm based on the Least Squares Method, as presented in Eq. (2), is applied to achieve an optimum fit between $P_m(D)$ and $P_t(D)$, and then the fraction of the coarse basalt aggregates are determined. The PSDs of the target and designed curve of UHPFRC matrix are shown in Fig. 1.

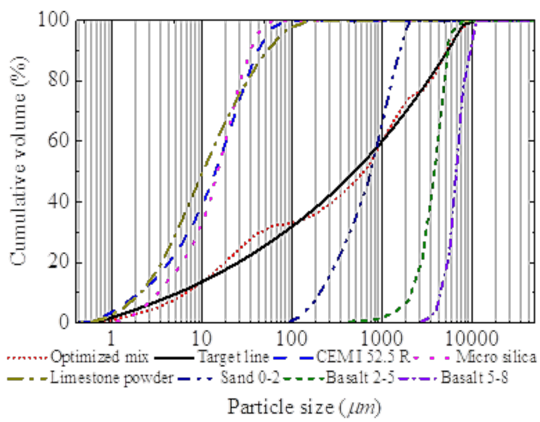

Fig. 1 PSD of raw materials and designed UHPFRC matrix

2.2 Mixing and casting procedures

The following mixing procedure was adopted for the UHPFRC matrix at room temperature of about 20 ± 1 °C: dry mixing of all powders and sands for 2 min; adding 75% water and mixing for 2 min; adding the superplasticizer and the remaining water; mixing for 4 min and then adding the steel fibers; adding the basalt aggregates and mixing for 3 min.

After mixing, the UHPFRC mixture was poured into the molds, and then the specimens were covered with plastic sheets to prevent moisture evaporation. They were demolded after 24 hours and cured in water under room temperature for an additional 27 days. All specimens were tested after the age of 28 days.

2.3 Testing methods

100×100×100 mm^3 cubic moulds were used for the tension and compression tests. The compressive and tensile splitting strengths of the UHPFRC samples were measured based on EN 12390-3 [18] and EN 12390-6 [19], respectively.

100×100×500 mm^3 beams were casted for testing the flexural strength. Three-point bending tests were conducted with the hydraulic testing machine, the span length was 400 mm and the load rate was 0.2 mm/min [20]. Two linear variable differential transducers (LVDTs) were used for measuring the mid-point deflections

3. Results and discussion

3.1 Tensile and compressive strengths

The splitting tensile and compressive strengths of the UHPFRC with fiber content V_f = 0%, 1% and 2% are given in Fig.2. As can be observed in the figure, the splitting tensile strength σ_t increase considerably with the fiber content. To be more specific, 44% and 97% increases in σ_t are observed for the UHPFRC incorporating 1% and 2% steel fibers, respectively, compared to that of the mixture without fibers. Additionally, it is observed that the UHPFRC cubes with fibers do not failed into two pieces during the splitting tension tests, which is attributed to the fibers' crack bridging effect and the strong bond between the fibers and the UHPFRC matrix [10].

Differing with the effects on the tensile strength, the addition of steel fibers has slight influences on the compressive strength σ_c of the UHPFRC. The σ_c of the V_f = 0%, 1% and 2% UHPFRC are around 138 MPa, 149 MPa and152 MPa, respectively. Additionally, these ultra-high compressive strength values also confirm the effectiveness of the mixture design in this study, i.e. with the Brouwers design method, the strength requirement of UHPFRC can be achieved when coarse basalt aggregates are used as replacement for the fine particles.

Moreover, the failure mode of the UHPFRC are distinct between the cubes with and without steel fibers. The V_f = 0% UHPFRC experienced a sudden and explosive damage, while the V_f = 1% and 2% UHPFRC cubes did not break into pieces after failure thanks to the connection of the fibers. These significant enhancement in the tensile strength and limited increases in the compressive strength are in agreement with the previous study [10].

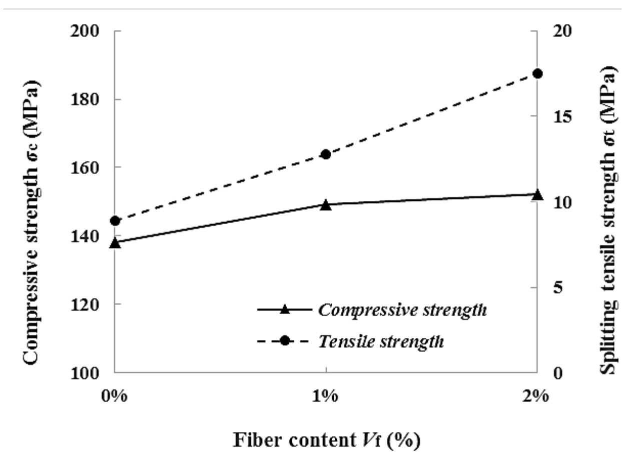

Fig. 2 Compressive and tensile strengths of the UHPFRC

3.2 Flexural strength and energy

The flexural behaviors of the UHPFRC mixtures with different fiber contents are significantly different, as shown in Fig.3. Under the three point bending, the V_f = 0% UHPFRC exhibits a sudden drop in load carrying capacity after reaching the peak load, as opposed to the gradual failure of the

UHPFRC beams reinforced with fibers. Strain-hardening is observed for the V_f = 2% UHPFRC, i.e. the flexural load increases after the first cracking of the UHPFRC beam. Conversely, the curve of V_f = 1% UHPFRC exhibits a steeper drop after the first crack occurs, and the beam presents a strain softening behavior with decreased flexural loads afterwards.

Furthermore, the peak flexural load and the flexural energy of UHPFRC are found to increase with the fiber content (Fig.4). The flexural energy is calculated by estimating the area under the flexural load-deflection curve in Fig.3. 14% and 30% increases in the peak flexural load are observed for the V_f = 1% and 2% UHPFRC, respectively, compared to that of the V_f = 0% UHPFRC. In addition, the enhancement of the flexural energy caused by the fibers is much more obvious. The V_f = 1% and 2% UHPFRC beams show approximately 35 and 38 times higher flexural energies than that of the V_f = 0% counterpart. With the incorporation of the steel fibers, the UHPFCR beam possesses a more effective control for the growth of micro-cracks into macro-cracks, and hence increases the load carrying capacity and toughness of the beam [10].

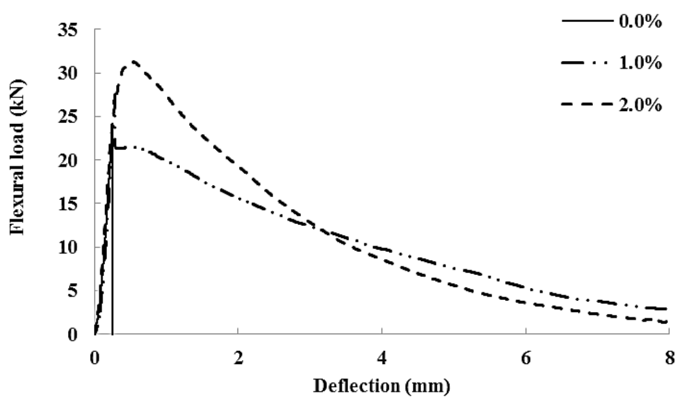

Fig. 3 Flexural load-deflection curves of the UHPFRC

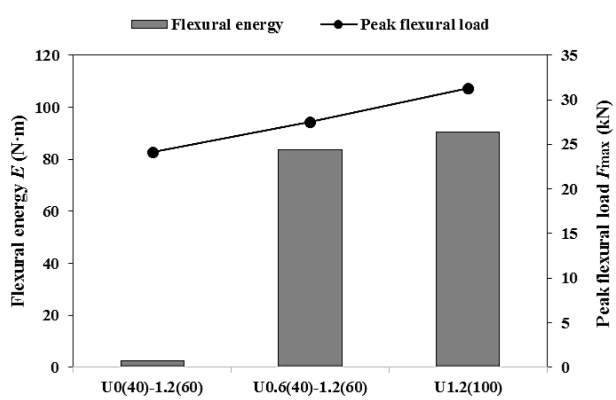

Fig. 4 Flexural load and energy of the UHPFRC

3.3 Cracking process

The cracking pattern of the UHPFRC with 0%, 1% and 2% fibers under three point bending are given in Figs. 5-7, respectively. As expected, the UHPFRC beam without steel fibers experienced a catastrophic and brittle failure and the beam was separated into two parts after the bending test. On contrast, the UHPFRC beams with 1% and 2% fibers showed a more stable cracking process: no cracks were observed at the initial linear elastic loading stage, after which post-crack stage began; a crack initiated from the beam bottom and propagated upwards to the beam top surface with the increase of the bending load; the crack became wider and the beam finally failed into two parts. For the fiber reinforced beams, some fibers were observed to be pulled out from the UHPFRC matrix, the process of which contributed to the improvement of the flexural energy. Moreover, for the V_f = 2% UHPFRC beam, the propagation of the crack was more tortuous (see Fig.7b and c), and the final macro crack was more twisted compared with the almost straight crack in the V_f = 1% UHPFRC beam (see Fig.6c). This is associated with the more prominent stress redistribution effect provided by the fibers, considering that the V_f = 2% UHPFRC beam contains more concentrated fibers, and that the pull-out of one fiber could result in the increasing loads in the neighboring fibers. This tortuous cracking process further enhances the flexural energy of the V_f = 2% UHPFRC beam.

(a) Mian crack (b) Failure surface

Fig. 5 Failure pattern of V_f = 0% UHPFRC

(a) t=5 min (b) t= 15 min (c) t= 30 min (d) Failure surface

Fig. 6 Failure pattern of V_f = 1% UHPFRC

(a) t=5 min (b) t= 15 min (c) t= 35 min (d) Failure surface

Fig. 7 Failure pattern of V_f = 2% UHPFRC

4. Conclusions

UHPFRC with coarse basalt aggregates of a maximum size of 8 mm was developed in this paper. The tensile and compressive strengths of the designed UHPFRC were tested, the results of which showed that the strength requirement could be achieved by properly packing the granular constituents based on the Brouwers design method. Furthermore, the effects of fiber content on the tensile, compressive and flexural performance of the UHPFRC were investigated experimentally with fiber volume fractions V_f = 0%, 1% and 2%. It is observed form the study that the compressive strength of the UHPFRC is almost independent on the fiber content, while the tensile and the flexural strengths are significantly increased with the increase of the fiber content. And the cracking process is more tortuous for the UHPFRC beam with a higher fiber content, resulting in a further enhancement of the flexural energy. The designed UHPFRC in this study contributes to the reduction of the binder in the UHPFRC matrix, which brings both economic and environmental benefits. Moreover, this study also provides an important perspective for understanding the fibers effects on UHPFRC and thus promotes the technological application of UHPFRC in practical constructions.

5. References

[1] Yoo DY, Banthia N. Mechanical properties of ultra-high-performance fiber-reinforced concrete: A review. Cem Concr Compos 2016;73:267–80. doi:10.1016/j.cemconcomp.2016.08.001.

[2] Li PP, Yu QL, Brouwers HJH. Effect of coarse basalt aggregates on the properties of Ultra-high Performance Concrete (UHPC). Constr Build Mater 2018;170:649–59. doi:10.1016/j.conbuildmat.2018.03.109.

[3] Wille K, Naman AE, Parra-Montesinos GJ. Ultra - High Performance Concrete with Compressive Strength Exceeding 150 MPa (22ksi) : A Simpler Way. ACI Mater J 2011;108:46–53. doi:10.14359/51664215.

[4] Ma J, Orgass M, Dehn F, Schmidt D, Tue N V. Comparative Investigations on Ultra-High Performance Concrete with or without Coarse Aggregates. Proc Int Symp Ultra High Perform Concr 2004:205–12.

[5] Collepardi S, Coppola L, Troli R, Collepardi M. Mechanical properties of modified reactive powder concrete. ACI Spec Publ 1997;173:1–22.

[6] Nguyen DL, Ryu GS, Koh KT, Kim DJ. Size and geometry dependent tensile behavior of ultra-high-performance fiber-reinforced concrete. Compos Part B Eng 2014;58:279–92. doi:10.1016/j.compositesb.2013.10.072.

[7] SpaSojević A. Structural Implications of Ultra-High Performance Fibre-Reinforced Concrete in Bridge Design. ingénieur civil diplômée de l'Université de Niš, Serbie et, 2008.

[8] Banthia N, Sappakittipakorn M. Toughness enhancement in steel fiber reinforced concrete through fiber hybridization. Cem Concr Res 2007;37:1366–72. doi:10.1016/j.cemconres.2007.05.005.

[9] Wille K, El-Tawil S, Naaman AE. Properties of strain hardening ultra high performance fiber reinforced concrete (UHP-FRC) under direct tensile loading. Cem Concr Compos 2014;48:53–66. doi:10.1016/j.cemconcomp.2013.12.015.

[10] Abbas S, Soliman AM, Nehdi ML. Exploring mechanical and durability properties of ultra-high performance concrete incorporating various steel fiber lengths and dosages. Constr Build Mater 2015;75:429–41. doi:10.1016/j.conbuildmat.2014.11.017.

[11] Li PP, Yu QL. Responses and post-impact properties of ultra-high performance fibre reinforced concrete under pendulum impact. Compos Struct 2018;31:under review.

[12] Li PP, Yu QL, Brouwers HJH. Effect of PCE-type superplasticizer on early-age behaviour of ultra-high performance concrete (UHPC). Constr Build Mater 2017;153:740–50. doi:10.1016/j.conbuildmat.2017.07.145.

[13] Norm D. Methods of test for mortar for masonry – Part 3: Determination of consistence of fresh mortar (by flow table) (includes Amendments A1:2004 + A2:2006) English version of DIN EN 1015-3:2007-05 Prüfverfahren, 2007.

[14] Brouwers HJH, Radix HJ. Self-compacting concrete: Theoretical and experimental study. Cem Concr Res 2005;35:2116–36. doi:10.1016/j.cemconres.2005.06.002.

[15] Wang X, Wang K, Taylor P, Morcous G. Assessing particle packing based self-consolidating concrete mix design method. Constr Build Mater 2014;70:439–52. doi:10.1016/j.conbuildmat.2014.08.002.

[16] Yu QL, Spiesz P, Brouwers HJH. Development of cement-based lightweight composites - Part 1: Mix design methodology and hardened properties. Cem Concr Compos 2013;44:17–29. doi:10.1016/j.cemconcomp.2013.03.030.

[17] Yu R. Development of sustainable protective Ultra-High Performance Fibre Reinforced Concrete (UHPFRC). Eindhoven University of Technology, 2015.

[18] Comité Européen de Normalisation. Testing hardened concrete - Part 3: Compressive strength of test specimens. Eur Stand EN 12390–3 2009.

[19] CEN. EN 12390-6:2000 Testing hardened concrete - Part 6: Tensile splitting strength of test specimens. 2000;44:1–8.

[20] RILEM TC 162-TDF. Recommendations of RILEM TC 162-TDF: Test and design methods for steel fibre reinforced concrete: bending test. Mater Struct 2002;35:579–82. doi:10.1617/14007.